Journal of Inorganic and General Chemistry
ZAAC
Zeitschrift für anorganische und allgemeine Chemie
DOI: 10.1002/zaac.202000394
ARTICLE

Homodinuclear Rh^{I} and Ir^{I} Complexes Derived from Imidazolium-Benzimidazolates

Kunal Kureja,[a] Julian Zinke,[a] Clemens Bruhn,[a] and Ulrich Siemeling*[a]

Dedicated to Prof. Christoph Janiak on the Occasion of his 60th Birthday

The reactions of [M(μ-Cl)(COD)]$_2$ (M=Rh, Ir) with the conjugated mesomeric betaines 2-(3-methyl-1-imidazolium)-benzimidazolate (**1a**H), 2-(3-isopropyl-1-imidazolium)-benzimidazolate (**1b**H) and 2-(3-*tert*-butyl-1-imidazolium)-benzimidazolate (**1c**H) in equilibrium with their carbenic tautomers **1'a**H, **1'b**H and **1'c**H were investigated. In the case of **1a**H and **1b**H, the homodinuclear complexes [MCl(COD){M(μ-**1'a**)(COD)}] and [MCl(COD){M(μ-**1'b**)(COD)}] were obtained, whose anionic NHC ligand **1'a**$^-$ or **1'b**$^-$ bridges the metal centres in a $\kappa^1N:\kappa^1N$ mode, while binding the M(COD) moiety in a *C*,*N*-chelating mode. For M=Ir, [IrCl(COD){Ir(μ-**1''b**)(COD)}] containing the "abnormal" NHC isomer **1''b**$^-$ was observed as a side product. In the case of **1'c**H, [{RhCl(COD)}$_2$(μ-**1c**H)] containing a $\kappa^1N:\kappa^1N$ benzimidazolato ligand was obtained for M=Rh, while for M=Ir the reaction furnished [IrCl(COD){Ir(μ-**1''c**)(COD)}], which contains the anionic "abnormal" NHC ligand **1''c**$^-$. This difference in behaviour is rationalised by the propensity of iridium(I) for oxidative addition, which in the present case involves a C–H bond of the dangling formamidium unit of [{IrCl(COD)}$_2$(μ-**1c**H)] to afford [Ir^{I}Cl(COD){Ir^{III}HCl(μ-**1''c**)(COD)}], followed by reductive elimination of HCl. The crystal structures of the new complexes were determined by single-crystal X-ray diffraction, except for [IrCl(COD){Ir(μ-**1'a**)(COD)}], where by serendipity the closely related mononuclear complex [Ir(**1'a**)(COD)] was structurally characterised instead.

Introduction

Imidazolium-benzimidazolates (**1**H) are readily available conjugated mesomeric betaines (CMBs),[1] which were recently established by us as convenient sources of donor-functionalised N-heterocyclic carbenes (NHCs).[2] Their "instant carbene" behaviour can be ascribed to a betaine–carbene tautomerisation (**1**H⇆**1'**H; Scheme 1), which was first recognised for the analytical reagent Nitron.[3–5]

In our previous work we have described mononuclear Ni^{II} chelates [NiCp(**1'**)],[2a] which contain deprotonated, and hence anionic, amido-NHC ligands,[6,7] viz. **1'**$^-$, and are easily obtained by reacting **1**H with nickelocene. Their oxidation afforded the corresponding cations [NiCp(**1'**)]$^+$, showing that **1'**$^-$ can support the unusual oxidation state Ni^{III}.[2b] The mononuclear chelates [NiCp(**1'**)] also provided ready access to heterodinuclear and heterotrinuclear complexes, viz. [CuBr{NiCp(μ-**1'**)}], [RhCl(COD){NiCp(μ-**1'**)}] (COD = $\eta^2:\eta^2$-cycloocta-1,5-diene) and [ZnI$_2${NiCp(μ-**1'**)}$_2$], in each case utilising the imine-type nitrogen atom of [NiCp(**1'**)] for coordination. The work described here addresses the synthesis of homodinuclear complexes of the type [MCl(COD){M(μ-**1'**)(COD)}] (M=Rh, Ir).

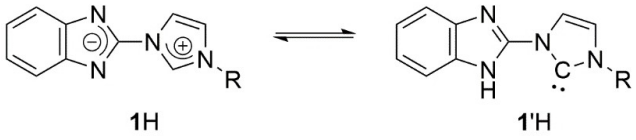

Scheme 1. CMBs of type **1**H in equilibrium with their carbenic tautomers **1'**H; substituents used in this work: R=Me (**a**), *i*Pr (**b**), *t*Bu (**c**).

Results and Discussion

Scheme 2 summarises the synthesis of the metal complexes of this study.

The reaction of **1a**H or **1b**H with [Rh(μ-Cl)(COD)]$_2$ afforded a mixture of the corresponding dinuclear complex [RhCl(COD){Rh(μ-**1'**)(COD)}] and the hydrochloride **1**H$_2$Cl, which unfortunately could not be separated. Two equivalents of the CMB were needed for full conversion, since **1**H also acts as a base in this process, "mopping up" the HCl produced in the formation of the Rh(μ-**1'**)(COD) unit. In the case of **1c**H, no deprotonation occurred and the $\kappa^1N:\kappa^1N$ benzimidinato complex [{RhCl(COD)}$_2$(μ-**1c**H)] was obtained in 58% yield, when the starting materials were used in a stoichiometric ratio of 1:1. When the reactions of **1a**H or **1b**H were performed in the presence of an additional base such as K_2CO_3,[8] the yields of [RhCl(COD){Rh(μ-

[a] *K. Kureja, J. Zinke, C. Bruhn, Prof. Dr. U. Siemeling*
Institute of Chemistry
University of Kassel
Heinrich-Plett-Str. 40, 34132 Kassel, Germany
Fax: +49-561-8044777
E-mail: siemeling@uni-kassel.de

Supporting information for this article is available on the WWW under https://doi.org/10.1002/zaac.202000394

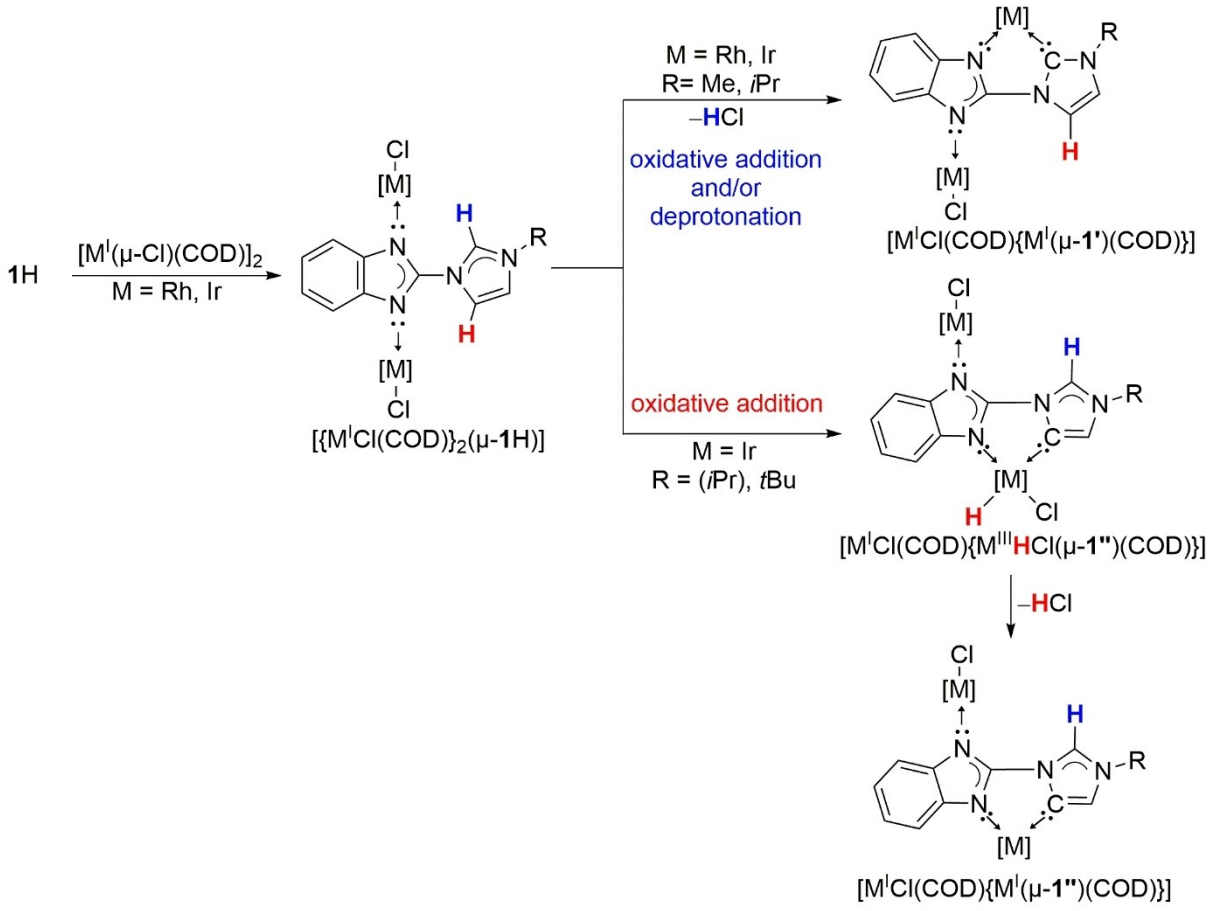

Scheme 2. Synthesis of the metal complexes of this study ([M] = M(COD); formal charges omitted for clarity). All reactions were performed in refluxing dichloromethane. HCl was removed with Ag_2O. The $\kappa^1N{:}\kappa^1N$ benzimidinato complex [{MCl(COD)}$_2$(μ-**1**H)] was isolated as the final product for M=Rh and R = *t*Bu (i.e. with **1c**H) and is assumed as an intermediate in all other cases, with the site and nature of the follow-up reactions being indicated in colour.

1'a)(COD)}] and [RhCl(COD){Rh(μ-**1'b**)(COD)}] were still only moderate at most. A better way to obtain these dinuclear Rh^I complexes turned out to be the "silver base route" established by Lin,[9,10] utilising Ag_2O for the deprotonation of the imidazolium unit and concomitant formation of a corresponding coordinatively labile silver(I) NHC complex. This approach afforded [RhCl(COD){Rh(μ-**1'a**)(COD)}] and [RhCl(COD){Rh(μ-**1'b**)(COD)}] in yields of at least 70%, when a moderate excess of Ag_2O was used (1.5 equivalents). This approach failed with **1c**H, where [{RhCl(COD)}$_2$(μ-**1c**H)] was furnished even under more forcing conditions (heating to reflux for several days), irrespective of the presence of Ag_2O in stoichiometric ratios of up to 2 equivalents. [RhCl(COD){Rh(μ-**1'a**)(COD)}] and [{RhCl(COD)}$_2$(μ-**1c**H)] were structurally characterised by single-crystal X-ray diffraction (XRD; Figures 1 and 2). The latter complex contains a functionalised bridging $\kappa^1N{:}\kappa^1N$ benzimidazolato ligand without additional chelation, which is rarely observed in the chemistry of benzimidazole-based ligands.[11]

The structure of these complexes in solution is essentially identical to that in the solid state according to an NMR spectroscopic analysis. The two COD ligands present in [RhCl(COD){Rh(μ-**1'a**)(COD)}] and [RhCl(COD){Rh(μ-**1'b**)(COD)}] give rise to eight ^{13}C NMR signals for the CH_2 units in each case. Their CH units give rise to doublets due to coupling to ^{103}Rh with $^1J_{RhC}$ values ranging from ca. 7–13 Hz. Only seven of the expected eight doublets were observed in each case. A Rh–$C_{carbene}$ doublet ($^1J_{RhC}$ = 53.8 Hz) was observed for [RhCl(COD){Rh(μ-**1'b**)(COD)}] at δ = 172.7 ppm, but could not be detected for the methyl congener, which can be ascribed to the significantly poorer solubility of the latter. In the ^{1}H NMR spectrum, the signal observed at lowest field (δ = 10.49 and 10.55 ppm for the μ-**1'a** and μ-**1'b** complex, respectively) is due to a proton of the $(CH)_2$ backbone of the NHC moiety. This signal is downfield-shifted by ca. 2 ppm in comparison to the corresponding CMB **1a**H or **1b**H. The molecular structure of [RhCl(COD){Rh(μ-**1'a**)(COD)}] reveals that this substantial downfield shift is most likely due to an intramolecular anagostic CH···Rh^I interaction (Rh1–H3 2.65 Å, Rh1–H3–C3 127°).[12] The ^{1}H NMR spectrum of [{RhCl(COD)}$_2$(μ-**1c**H)] shows a low-field signal at δ = 11.47 ppm for the N_2CH unit of the formamidinium moiety, which is down-field-shifted by ca. 2 ppm with respect to **1c**H. In the solid state this H atom appears to be involved in

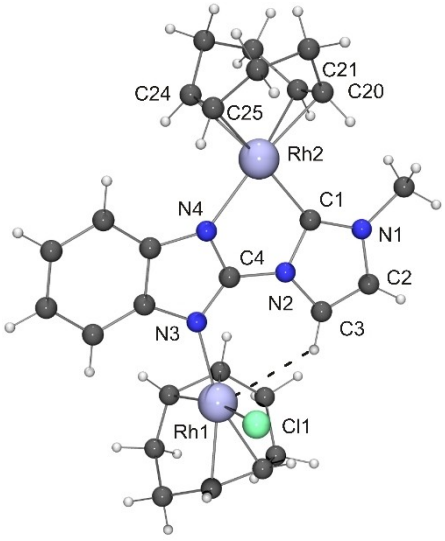

Figure 1. Molecular structure of [RhCl(COD){Rh(μ-**1′a**)(COD)}]·2CHCl$_3$ in the crystal. The solvent molecules have been omitted for clarity. The CH···Rh^{I} contact compatible with an anagostic interaction is indicated by a dashed line. Selected bond lengths/Å: Rh2–C20 2.162(3), Rh2–C21 2.130(2), Rh2–C24 2.204(3), Rh2–C25 2.190(2).

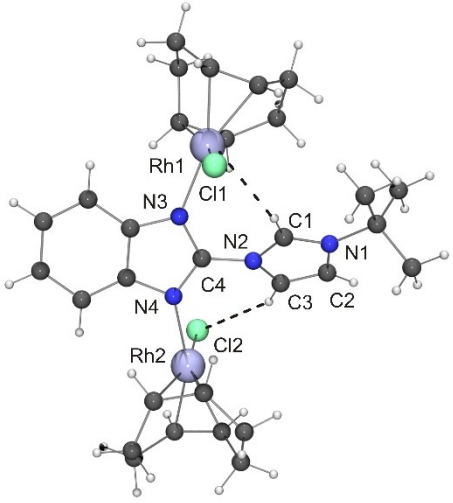

Figure 2. Molecular structure of [{RhCl(COD)}$_2$(μ-**1cH**)]·CH$_2$Cl$_2$ in the crystal. The solvent molecule has been omitted for clarity. The CH···Rh^{I} and CH···Cl contacts compatible respectively with anagostic and hydrogen bond interactions are indicated by dashed lines.

an anagostic CH···Rh^{I} (Rh1–H1 2.79 Å, Rh1–H1–C1 108°) and an intramolecular CH···Cl hydrogen bond interaction[13] (Cl1–H1 2.53 Å, Cl1–H1–C1 156°) with the chlorido ligand at Rh1. The second CH···Rh^{I} contact present in this complex (Rh2–H3 2.97 Å, Rh1–H3–C3 113°) is borderline for an anagostic interaction. Nevertheless, the ^{1}H NMR signal due to this CH unit at $\delta =$ 10.00 ppm is substantially down-field shifted by ca. 1.4 ppm with respect to **1c**H. We note that, in addition to its rather long CH···Rh^{I} contact, this CH unit is also involved in a weak intramolecular CH···Cl hydrogen bond interaction in the solid state (Cl2–H3 2.63 Å, Cl2–H3–C3 148°). The two COD ligands of [{RhCl(COD)}$_2$(μ-**1c**H)] give rise to four ^{13}C NMR signals each for their CH and CH$_2$ units, indicating that the COD ligands are equivalent on the NMR time scale.

Our futile attempts to synthesise [RhCl(COD){Rh(μ-**1′c**)(COD)}] prompted us to test the analogous iridium chemistry. Consequently, the "silver base route" procedure established for the preparation of [RhCl(COD){Rh(μ-**1′a**)(COD)}] and [RhCl(COD){Rh(μ-**1′b**)(COD)}] was applied to **1c**H and [Ir(μ-Cl)(COD)]$_2$. This afforded the dinuclear complex [IrCl(COD){Ir(μ-**1′′c**)(COD)}] in 73% yield, which was structurally characterised by XRD (Figure 3). This product was also obtained in the absence of Ag$_2$O, albeit in lower yield and contaminated with the hydrochloride **1c**H$_2$Cl.

This complex does not contain the anionic NHC ligand **1′c**$^{-}$, but instead the isomeric "abnormal" NHC (aNHC) **1′′c**$^{-}$.[14] The Ru^{II} complex [Ru(**1′′c**H)$_2$(PPh$_3$)$_2$]Cl$_2$ containing the protonated, and hence electroneutral, form **1′′c**H as chelate ligand had been described already in our previous work.[2a] aNHC formation is known to be favoured by steric congestion.[14,15] Note that iridium benzimidazolato–aNHC *C*,*N*-chelates have been developed as catalysts for the hydrogenation of aldehydes and carbon dioxide.[16] The ^{13}C NMR signal due to the C$_{carbene}$ atom of [IrCl(COD){Ir(μ-**1′′c**)(COD)}] was observed at $\delta = 156.6$ ppm in CD$_2$Cl$_2$. The formally cationic N$_2$CH unit of the "abnormal" carbene moiety gives rise to a diagnostic low-field ^{1}H NMR signal at $\delta = 11.26$ ppm in CD$_2$Cl$_2$, which compares well with the N$_2$CH signal of [{RhCl(COD)}$_2$(μ-**1c**H)] at $\delta = 11.47$ ppm. Again, an anagostic interaction is evident from the crystal structure (Ir1–H1 2.78 Å, Ir1–H1–C1 126°). Irrespective of the use of Ag$_2$O, crude [IrCl(COD){Ir(μ-**1′′c**)(COD)}] contained small amounts of an impurity which showed a ^{1}H NMR signal at conspicuously high field ($\delta = -14.73$ ppm), indicative of a hydrido complex. We

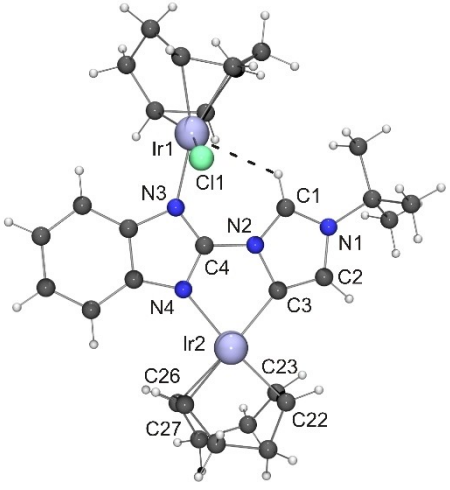

Figure 3. Molecular structure of [IrCl(COD){Ir(μ-**1′′c**)(COD)}]·CH$_2$Cl$_2$ in the crystal. The solvent molecule has been omitted for clarity. The CH···Ir^{I} contact compatible with an anagostic interaction is indicated by a dashed line. Selected bond lengths/Å: Ir2–C23 2.189(8), Ir2–C24 2.143(9), Ir2–C27 2.125(8), Ir2–C28 2.112(8).

surmise that the reaction of **1c**H with $[M(\mu\text{-Cl})(COD)]_2$ (M=Rh, Ir) affords $[\{MCl(COD)\}_2(\mu\text{-}\mathbf{1c}H)]$, which is isolated as the final product for M=Rh, but undergoes a follow-up reaction in the case of M=Ir, namely an intramolecular C–H activation of the formamidinium unit (oxidative addition at Ir^{I}; Scheme 2). Due to the neighbouring bulky *t*Bu substituent, this cyclometallation does not involve the N_2CH unit, but the proximal CH unit of the $(CH)_2$ moiety, thus leading to the hydrido complex $[Ir^{I}Cl(COD)\text{-}\{Ir^{III}HCl(\mu\text{-}\mathbf{1''c})(COD)\}]$ with the "abnormal" carbene ligand **1''c**$^-$. Finally, reductive elimination of HCl (efficiently removed by Ag_2O) affords [IrCl(COD){Ir(μ-**1''c**)(COD)}]. Oxidative additions are known to be much more facile for Ir^{I} than for Rh^{I},[17] and this has been confirmed also for the oxidative addition of imidazolium C–H bonds.[18]

The analogous reaction with the sterically least encumbered CMB **1a**H with $[Ir(\mu\text{-Cl})(COD)]_2$ afforded the "normal" NHC complex [IrCl(COD){Ir(μ-**1'a**)(COD)}], which was isolated in 65% yield. Its NMR spectroscopic features are similar to those of the corresponding Rh analogue. Eight ^{13}C NMR signals each were observed for the CH and CH_2 units of the two COD ligands. In contrast to the Rh analogue, it was possible in this case to detect the ^{13}C NMR signal due to the $C_{carbene}$ atom (δ = 172.4 ppm). In the ^{1}H NMR spectrum, the signal observed at lowest field (δ = 9.96 ppm) is due to a proton of the $(CH)_2$ backbone of the NHC moiety, which very likely is involved in an anagostic CH···Ir^{I} interaction similar to that discussed above for the structurally characterised Rh^{I} analogue. The reaction of **1b**H with $[Ir(\mu\text{-Cl})(COD)]_2$ also led to the "normal" NHC complex [IrCl(COD){Ir(μ-**1'b**)(COD)}] (56% yield), whose NMR spectroscopic features are very similar to those of the methyl congener just described. From the structure of this compound (Figure 4) the anagostic interaction just suggested for the methyl congener is clearly evident (Ir1–H3 2.68 Å, Ir1–H3–C3 126°). Similar to the reaction of **1c**H described above, the ^{1}H NMR spectrum of the crude product indicated the presence of small amounts of a hydrido complex (high-field signal at δ = −13.02 ppm), which was removed by crystallisation. Fortuitously, crystallisation afforded a few single crystals also of the isomeric [IrCl(COD){Ir(μ-**1''b**)(COD)}] (Figure 5), whose presence in the crude product had not been obvious from the NMR spectra. Similar to [IrCl(COD){Ir(μ-**1''c**)(COD)}], the N_2CH unit is involved in an anagostic interaction (Ir1–H1 2.73 Å, Ir1–H1–C1 128°).

One of our numerous attempts to obtain single crystals of [IrCl(COD){Ir(μ-**1'a**)(COD)}] suitable for XRD serendipitously afforded a few crystals of the mononuclear chelate [Ir(**1'a**)(COD)] (Figure 6).

The structures of the complexes of this study share a number of characteristic features. The five-membered ring chelate complexes exhibit very similar N–M–$C_{carbene}$ angles (78.1–79.4°). The M–Cl bond lengths of the dinuclear complexes lie in the narrow range from 2.34–2.40 Å, which is due to the

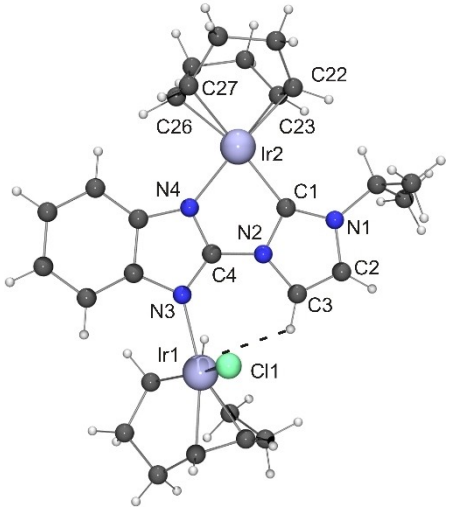

Figure 4. Molecular structure of $[IrCl(COD)\{Ir(\mu\text{-}\mathbf{1'b})(COD)\}]\cdot C_2H_4Cl_2$ in the crystal. The solvent molecule has been omitted for clarity. The CH···Ir^{I} contact compatible with an anagostic interaction is indicated by a dashed line. Selected bond lengths/Å: Ir2–C22 2.123(4), Ir2–C23 2.113(4), Ir2–C26 2.159(4), Ir2–C27 2.181(5).

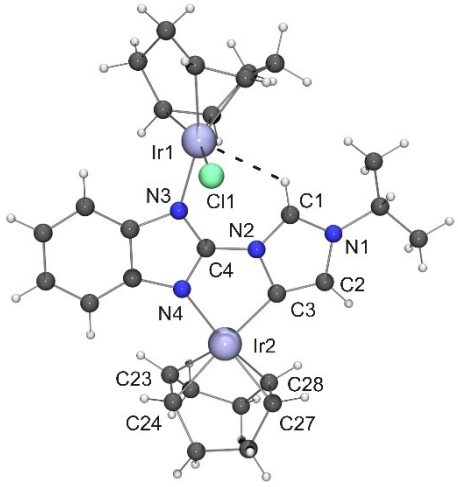

Figure 5. Molecular structure of [IrCl(COD){Ir(μ-**1''b**)(COD)}] in the crystal. The CH···Ir^{I} contact compatible with an anagostic interaction is indicated by a dashed line. Selected bond lengths/Å: Ir2–C22 2.104(12), Ir2–C23 2.120(12), Ir2–C26 2.148(11), Ir2–C27 2.158(11).

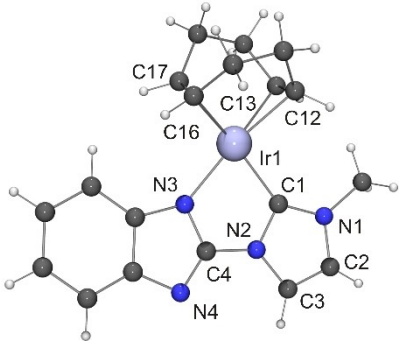

Figure 6. Molecular structure of [Ir(**1'a**)(COD)] in the crystal. Only one of the two independent molecules present in the asymmetric unit is shown. Selected bond lengths/Å: Ir1–C12 2.131(5), Ir1–C13 2.138(5), Ir1–C16 2.163(6), Ir1–C17 2.184(5).

very similar covalent radii of Rh and Ir (1.42 and 1.41 Å, respectively).[19] This similarity is also reflected by the M–N bond lengths, whose average value is 2.10 Å for the Rh^{I} and 2.08 Å for the Ir^{I} complexes, and by the $M–C_{carbene}$ bond lengths, which are all indistinguishable within experimental error (average value 2.05 Å) and slightly, but significantly, shorter than the M–N bond lengths, as has been noted before for the Ni^{II} chelates [NiCp(**1′**)].[2] These and further pertinent bond lengths are collected in Table 1.

The lengths of the two M–N bonds of the dinuclear complexes are indistinguishable within experimental error in each case, indicating that a differentiation between putative N_{amido} and N_{imine} atoms is not meaningful. This is further supported by the fact that in each case the lengths of the two C–N bonds in the benzimidazole-based N_2C unit are indistinguishable within experimental error, too. The average value of these C–N bonds is 1.33 Å, which is intermediate between the values typical of $C(sp^2)–N(sp^2)$ single (1.41 Å) and double bonds (1.28 Å),[20] indicating efficient π delocalisation in this N_2C unit. In contrast, the mononuclear complex [Ir(**1′a**)(COD)] exhibits significantly different bond lengths (ca. 1.35 vs. ca. 1.30 Å), compatible with a coordinated N_{amido} and an uncoordinated N_{imine} atom. Note that the interannular C–N bonds range from ca. 1.39–1.41 Å for all complexes of this study, pointing to a very low degree of π delocalisation between the two heterocyclic rings in all cases. The M–C(COD) bonds of the metal centres contained in a five-membered chelate ring are slightly longer (by ca. 0.05 Å; see Figures 1 and 3–6) for the part of the diene that is *trans* to the carbene ligand, as expected from the pronounced *trans* influence[21] of NHC ligands.[22]

Conclusion

Depending on the metal, the reaction of **1c**H with [M(μ-Cl)(COD)]$_2$ (M=Rh, Ir) leads to completely different products, viz. the benziminato-bridged complex [{RhCl(COD)}$_2$(μ-**1c**H)] with a dangling formamidinium unit and the *C*,*N*-chelate [IrCl(COD){Ir(μ-**1′′c**)(COD)}] with an anionic aNHC ligand, which represent coordination modes hitherto unknown for ligands based on CMB system **1**H. This difference can be rationalised by the comparatively higher propensity of iridium(I) for oxidative addition, which in the present case involves a C–H bond of the dangling formamidinium unit of the assumed intermediate [{IrCl(COD)}$_2$(μ-**1c**H)]. Such a cyclometallation does not occur with the rhodium(I) analogue [{RhCl(COD)}$_2$(μ-**1c**H)]. Likewise, the rhodium(I) *C*,*N*-chelates [RhCl(COD){Rh(μ-**1′a**)(COD)}] and [RhCl(COD){Rh(μ-**1′b**)(COD)}] containing an anionic "normal" NHC ligand are most likely not formed by cyclometallation, but via deprotonation of the formamidinium N_2CH unit. An analogous formation of [RhCl(COD){Rh(μ-**1′c**)(COD)}] via deprotonation is obviously prevented by the bulky *t*Bu substituent, as has been observed before for pyrazolyl-NHC Rh^{I} chelates,[23] and the formation of a rhodium(I) *C*,*N*-chelate with the anionic aNHC ligand **1′′c**$^-$ via deprotonation does not occur due to the prohibitively low CH acidity of the "abnormal" precarbenic position of the formamidinium unit.[24]

Experimental Section

All reactions involving air-sensitive compounds were performed in an inert atmosphere (argon or dinitrogen) by using Schlenk techniques or a conventional glovebox. Starting materials were procured from standard commercial sources and used as received. **1a**H,[25] **1b**H[2a] and **1c**H[2a] were synthesised by following adapted versions of the published procedures. NMR spectra were recorded at ambient temperature with Varian NMRS-500 and MR-400 spectrometers operating at 500 and 400 MHz, respectively, for ^{1}H. Combustion analyses were carried out with a HEKAtech Euro EA-CHNS elemental analyser at the Institute of Chemistry, University of Kassel, Germany.

Synthesis of [RhCl(COD){Rh(μ-1′a)(COD)}]: A stirred suspension of **1a**H (99 mg, 0.50 mmol) and Ag_2O (174 mg, 0.75 mmol) in dichloromethane (20 mL) was refluxed for 1 h. [Rh(μ-Cl)(COD)]$_2$ (247 mg, 0.50 mmol) was added and refluxing continued for 1 h. The mixture was allowed to cool to room temperature and filtered through a Celite pad. The filtrate was reduced to dryness under vacuum. The

Table 1. Selected bond lengths/Å of the structurally characterised complexes of this study.

	$M–C_{carbene}$	M–N	M–Cl	$C–N_{Blm}$ [a]	$C–N_{Im}$ [b]	$C–N_{inter}$ [c]
[RhCl(COD){Rh(μ-**1′a**)(COD)}]	2.048(3)	2.091(2)[d]	2.3851(6)	1.325(3)	1.347(3)	1.397(3)
		2.104(2)		1.341(3)	1.380(3)	
[{RhCl(COD)}$_2$(μ-**1c**H)]		2.098(2)[d]	2.3671(7)	1.331(4)	1.328(4)	1.411(4)
		2.104(2)	2.3973(7)	1.329(4)	1.343(4)	
[IrCl(COD){Ir(μ-**1′′c**)(COD)}]	2.033(8)	2.095(6)[d]	2.357(2)	1.308(10)	1.343(10)	1.409(10)
		2.109(7)		1.328(10)	1.328(10)	
[IrCl(COD){Ir(μ-**1′b**)(COD)}]	2.057(4)	2.079(3)[d]	2.3596(11)	1.329(5)	1.362(5)	1.394(5)
		2.082(3)		1.345(5)	1.375(5)	
[IrCl(COD){Ir(μ-**1′′b**)(COD)}]	2.035(11)	2.073(10)[d]	2.339(3)	1.329(15)	1.362(16)	1.389(15)
		2.078(9)		1.342(14)	1.317(14)	
[Ir(**1′a**)(COD)][e]	2.065(5)	2.065(5)		1.355(7)	1.355(7)	1.410(7)
	2.060(5)	2.071(5)		1.297(7)	1.362(7)	1.410(7)
				1.353(7)	1.354(7)	
				1.296(7)	1.368(7)	

a) Bond lengths in the benzimidazole-based N_2C unit. b) Bond lengths in the imidazole-based N_2C unit. c) Interannular bond length. d) N atom of the five-membered chelate ring. e) Two independent molecules.

crude product thus obtained was purified by column chromatography (silica gel, ethyl acetate), which afforded a yellow microcrystalline solid. Yield 236 mg (72%). **^{1}H NMR** (CD_2Cl_2): δ = 10.49 (s, 1 H, NCHCHN), 8.34 (d, J = 8.1 Hz, 1 H, C_6H_4), 7.19 (m, 1 H, C_6H_4), 7.11–7.05 (m, 2 H, C_6H_4), 6.99 (s, 1 H, NCHCHN), 5.82–5.75, 5.75–5.67 (2 m, 2×1 H, CH_{COD}), 4.74–4.70 (m, 1 H, CH_{COD}), 4.67–4.61 (m, 3 H, CH_{COD}), 3.76–3.70 (m, 1 H, CH_{COD}), 3.61 (s, 3 H, Me), 3.51–3.47 (m, 1 H, CH_{COD}), 2.73–2.65 (m, 1 H, CH_2), 2.56–2.33 (m, 7 H, CH_2), 2.16–2.06 (m, 3 H, CH_2), 2.01–1.94 (m, 1 H, CH_2), 1.87–1.69 ppm (m, 3 H, CH_2). **^{13}C{^{1}H} NMR** (CD_2Cl_2): δ = 123.3 (NCHCHN), 122.6, 121.3 (2×C_6H_4), 119.1 (NCHCHN), 114.3 (C_6H_4), 94.0 (d, J_{CRh} = 6.6 Hz, CH_{COD}), 93.5 (d, J_{CRh} = 7.9 Hz, CH_{COD}), 85.4 (d, J_{CRh} = 11.6 Hz, CH_{COD}), 84.1 (d, J_{CRh} = 12.9 Hz, CH_{COD}), 76.3 (d, J_{CRh} = 12.3 Hz, CH_{COD}), 73.8 (d, J_{CRh} = 12.4 Hz, CH_{COD}), 73.2 (d, J_{CRh} = 12.6 Hz, CH_{COD}), 36.7 (CH_3), 33.2, 32.8, 32.6, 31.5, 31.3, 30.8, 30.2, 30.0 ppm (8×CH_2). $C_{27}H_{33}N_4ClRh_2$ (654.84): calcd. C 49.52, H 5.08, N 8.56%; found C 49.55, H 5.02, N 8.23%.

Synthesis of [RhCl(COD){Rh(μ-1′b)(COD)}]: The product was obtained as a yellow, microcrystalline solid (239 mg, 70%) from **1b**H (113 mg, 0.50 mmol), Ag_2O (174 mg, 0.75 mmol) and [Rh(μ-Cl)(COD)]$_2$ (247 mg, 0.50 mmol) by a procedure essentially identical to that described above for [RhCl(COD){Rh(μ-**1′a**)(COD)}]. **^{1}H NMR** (CD_2Cl_2): δ = 10.55 (s, 1 H, NCHCHN), 8.34 (d, J = 8.1 Hz, 1 H, C_6H_4), 7.20–7.05 (m, 4 H, NCHCHN and 3×C_6H_4), 5.77–5.65 (m, 2 H, CH_{COD}), 5.54 (s, 1 H, CH_{COD}), 4.72–4.60 (m, 2 H, CH_{COD}), 4.55 (s, 1 H, CH_{COD}), 3.96 (sept, J = 6.9 Hz, 1 H, C*H*Me$_2$), 3.75–3.69 (m, 1 H, CH_{COD}), 3.54–3.48 (m, 1 H, CH_{COD}), 2.72–2.59 (m, 1 H, CH_2), 2.54–2.32 (m, 5 H, CH_2), 2.15–1.69 (m, 10 H, CH_2), 1.51, 1.50 ppm (2 d, J = 6.8 Hz, 2×3 H, CH*Me*$_2$). **^{13}C{^{1}H} NMR** (CD_2Cl_2): δ = 172.7 (d, J_{CRh} = 53.8 Hz, $C_{carbene}$), 156.2 (N_3C), 143.1, 142.0 (2×C_6H_4), 122.5 (NCHCHN), 121.2, 119.9, 119.1 (3×C_6H_4), 117.3 (NCHCHN), 114.2 (C_6H_4), 93.1 (d, J_{CRh} = 8.0 Hz, CH_{COD}), 92.7 (d, J_{CRh} = 8.2 Hz, CH_{COD}), 85.3 (d, J_{CRh} = 11.5 Hz, CH_{COD}), 84.0 (d, J_{CRh} = 11.9 Hz, CH_{COD}), 76.3 (m, CH_{COD}), 73.5 (d, J_{CRh} = 12.8 Hz CH_{COD}), 73.0 (d, J_{CRh} = 12.5 Hz CH_{COD}), 51.0 (C*H*Me$_2$), 33.1, 32.7, 32.6, 31.5, 31.2, 30.9, 30.2, 30.1 (8×CH_2), 24.1, 24.0 ppm (2×CH*Me*$_2$). $C_{29}H_{36}N_4ClRh_2{\cdot}CH_2Cl_2$ (766.82): calcd. C 46.99, H 4.99, N 7.31%; found C 46.22, H 5.15, N 7.29%.

Synthesis of [{RhCl(COD)}$_2$(μ-1cH)]: A solution of **1c**H (120 mg, 0.50 mmol) and [Rh(μ-Cl)(COD)]$_2$ (247 mg, 0.50 mmol) in dichloromethane (20 mL) was refluxed for 1 h. The mixture was allowed to cool to room temperature and filtered through a Celite pad. The filtrate was reduced to dryness under vacuum and the residue recrystallized from dichloromethane, which afforded the product as yellow needles. Yield 213 mg (58%). **^{1}H NMR** (CD_2Cl_2): δ = 11.47 (s, 1 H, N_2CH), 10.00 (s, 1 H, NCHCHN), 8.24–8.22 (m, 2 H, C_6H_4), 7.73 (s, 1 H, NCHCHN), 7.33–7.31 (m, 2 H, C_6H_4), 4.69–4.62, 4.59–4.52, 3.68–3.61, 3.11–3.04 (4 m, 4×2 H, CH_{COD}), 2.71–2.60, 2.48–2.37, 2.22–2.12 (3 m, 3×2 H, CH_2), 1.97 (s, 9 H, CMe_3), 1.94–1.84 (m, 4 H, CH_2), 1.81–1.66 ppm (m, 6 H, CH_2). **^{13}C{^{1}H} NMR** (CD_2Cl_2): δ = 148.2 (N_3C), 144.5 (C_6H_4) 142.8 (N_2CH), 136.8 (NCHCHN), 122.8, 118.4 (2×C_6H_4), 100.7 (NCHCHN), 85.7, 84.3, 76.8, 76.6 (4×CH_{COD}), 62.0 (CMe_3), 33.1, 31.5, 31.1 (3×CH_2), 30.6 (CMe_3), 30.4 ppm (CH_2). $C_{30}H_{40}N_4Cl_2Rh_2{\cdot}CH_2Cl_2$ (766.82): calcd. C 45.50, H 5.17, N 6.85%; found C 45.34, H 5.26, N 6.66%.

Synthesis of [IrCl(COD){Ir(μ-1′a)(COD)}]: A stirred suspension of **1a**H (10 mg, 50 μmol) and Ag_2O (17 mg, 73 μmol) in dichloromethane (5 mL) was refluxed for 1 h. [Ir(μ-Cl)(COD)]$_2$ (25 mg, 0.50 μmol) was added and refluxing continued for 1 h. The mixture was allowed to cool to room temperature and filtered through a Celite pad. The filtrate was reduced to dryness under vacuum. The residue was washed with diethyl ether (2×5 mL) and subsequently taken up in dichloromethane (2 mL). Diethyl ether (15 mL) was added dropwise. The precipitate was filtered off and recrystallized by vapour diffusion of diethyl ether into a 1,2-dichloroethane solution, which afforded the product as red crystals. Yield 27 mg (65%). **^{1}H NMR** (CD_2Cl_2): δ = 9.96 (s, 1 H, NCHCHN), 8.16 (s, 1 H, C_6H_4), 7.22–7.11 (m, 3 H, C_6H_4), 6.91 (s, 1 H, NCHCHN), 5.63–5.49 (m, 2 H, CH_{COD}), 4.51–4.35 (m, 2 H, CH_{COD}), 4.18 (m, 2 H, CH_{COD}), 3.62 (s, 3 H, Me), 3.45–3.35 (m, 2 H, CH_{COD}), 3.15–3.08 (m, 1 H, CH_2), 2.45–2.14 (m, 9 H, CH_2), 1.97–1.83 (m, 3 H, CH_2), 1.78–1.67, 1.65–1.54, 1.52–1.35 ppm (3 m, 3×1 H, CH_2). **^{13}C{^{1}H} NMR** (CD_2Cl_2): δ = 172.4 ($C_{carbene}$), 143.1 (N_3C), 141.6, 140.6, 124.2 (3×C_6H_4), 123.6 (NCHCHN), 121.9, 119.9, 119.6 (3×C_6H_4), 114.5 (NCHCHN), 82.0, 81.5, 70.4, 69.3, 59.0, 58.9, 58.2, 57.8 (8×CH_{COD}), 36.7 (Me), 34.2, 33.8, 33.1, 32.2, 32.1, 31.7, 31.2, 31.0 ppm (8×CH_2). $C_{27}H_{33}N_4ClIr_2$ (833.46): calcd. C 38.91, H 3.99, N 6.72%; found C 38.49, H 4.08, N 6.70%.

Synthesis of [IrCl(COD){Ir(μ-1′b)(COD)}]: The product was obtained as red crystals (24 mg, 56%) from **1b**H (11 mg, 50 μmol), Ag_2O (17 mg, 73 μmol) and [Ir(μ-Cl)(COD)]$_2$ (25 mg, 50 μmol) by a procedure essentially identical to that described above for [IrCl(COD){Ir(μ-**1′a**)(COD)}]. **^{1}H NMR** (CD_2Cl_2): δ = 10.04 (s, 1 H, NCHCHN), 8.16 (d, J = 7.6 Hz, 1 H, C_6H_4), 7.23–7.14 (m, 3 H, C_6H_4), 7.08 (s, 1 H, NCHCHN), 5.62–5.56, 5.55–5.49, 4.50–4.46, 4.42–4.38 (4 m, 4×1 H, CH_{COD}), 4.17–4.09 (m, 3 H, C*H*Me$_2$ and CH_{COD}), 3.44–3.38 (m, 1 H, CH_{COD}), 3.18–3.14, 2.49–2.41 (2 m, 2×1 H, CH_2), 2.35–2.15 (m, 7 H, CH_2), 1.97–1.81 (m, 4 H, CH_2), 1.79–1.69 (m, 1 H, CH_2), 1.66–1.58 (m, 1 H, CH_2), 1.52 (d, J = 6.5 Hz, 6 H, CH*Me*$_2$), 1.46–1.37 ppm (m, 1 H, CH_2). **^{13}C{^{1}H} NMR** (CD_2Cl_2): δ = 170.8 ($C_{carbene}$), 143.2 (N_3C), 141.5, 140.6 (2×C_6H_4), 123.6 (NCHCHN), 121.8, 120.8, 119.6 (3×C_6H_4), 118.4 (NCHCHN), 114.5 (C_6H_4), 80.9, 80.5, 70.4, 69.2, 59.1, 58.8, 57.8, 57.4 (8×CH_{COD}), 51.1 (C*H*Me$_2$), 34.0, 33.7, 33.1 (3×CH_2), 32.2 (CH*Me*$_2$), 31.7, 31.1 (two very closely spaced signals), 24.0, 23.9 ppm (5×CH_2). $C_{29}H_{37}N_4ClIr_2$ (861.52): calcd. C 40.43, H 4.33, N 6.50%; found C 39.60, H 4.59, N 5.95%.

Synthesis of [IrCl(COD){Ir(μ-1″c)(COD)}]: The product was obtained as red crystals (32 mg, 73%) from **1c**H (12 mg, 50 μmol), Ag_2O (17 mg, 73 μmol) and [Ir(μ-Cl)(COD)]$_2$ (25 mg, 50 μmol) by a procedure essentially identical to that described above for [IrCl(COD){Ir(μ-**1′a**)(COD)}]. **^{1}H NMR** (CD_2Cl_2): δ = 11.26 (s, 1 H, N_2CH), 8.10–8.08 (m, 1 H, C_6H_4), 7.26–7.15 (m, 3 H, C_6H_4), 6.74 (s, 1 H, $C_{carbene}CH$), 5.23–5.16, 5.14–5.08, 4.57–4.53, 4.42–4.37 (4 m, 4×1 H, CH_{COD}), 3.92–3.84 (m, 2 H, CH_{COD}), 3.55–3.49, 3.21–3.16 (2 m, 2×1 H, CH_{COD}), 2.54–2.43, 2.40–2.31 (2 m, 2×1 H, CH_2), 2.29–2.14 (m, 6 H, CH_2), 1.96–1.91 (m, 2 H, CH_2), 1.85–1.78 (m, 4 H, CH_2), 1.75 (s, 9 H, CMe_3), 1.71–1.65, 1.47–1.37 (2 m, 2×1 H, CH_2). **^{13}C{^{1}H} NMR** (CD_2Cl_2): δ = 156.6 ($C_{carbene}$), 142.3 (N_3C), 141.5, 140.0 (2×C_6H_4), 130.1 (N_2CH), 122.9, 121.5, 120.9 (3×C_6H_4), 118.3 ($C_{carbene}CH$), 114.6 (C_6H_4), 76.7, 76.3, 70.7, 68.8 (4×CH_{COD}), 65.6 (CMe_3), 58.8, 58.6, 57.1, 56.8 (4×CH_{COD}), 33.3, 32.4, 32.1, 31.7, 31.3 (5×CH_2), 31.2 (2×CH_2, as judged from the relative intensity of the signal), 31.0 (CH_2), 29.8 (CMe_3). $C_{30}H_{39}N_4ClIr_2$ (875.54): calcd. C 41.15, H 4.49, N 6.40%; found C 41.26, H 4.67, N 6.13%.

X-ray Crystallography: For each data collection a single crystal was mounted on a micro-mount at 100(2) K and all geometric and intensity data were taken from this sample. Data collections were carried out on a Stoe IPDS2 diffractometer equipped with a 2-circle goniometer and an area detector in the case of [{RhCl(COD)}$_2$(μ-**1cH**)] CH_2Cl_2 and [IrCl(COD){Ir(μ-**1″b**)(COD)}], whereas a Stoe StadiVari diffractometer equipped with a 4-circle goniometer and a DECTRIS Pilatus 200 K detector was used for all other cases. The diffraction experiments were performed with Mo-K_α radiation (λ = 0.71073 Å) in all cases except [IrCl(COD){Ir(μ-**1″c**)(COD)}] CH_2Cl_2 and [Ir(**1′a**)(COD)], where Cu-K_α radiation (λ = 1.54186 Å) was used. The data sets were corrected for absorption, Lorentz and polarisation effects. The structures were solved by direct methods (SHELXT)[26] and refined using alternating cycles of least-squares refinements against F^2 (SHELXL2014/7).[26] C-bonded H atoms were included to the models in calculated positions, heteroatom-bonded H atoms have been found in the difference Fourier lists. All H atoms were treated with the 1.2 fold or 1.5 fold isotropic displacement

Table 2. X-ray crystallographic details.

	[RhCl(COD){Rh(μ-**1′a**)(COD)}]·2CHCl$_3$	[{RhCl(COD)}$_2$(μ-**1c**H)]·CH$_2$Cl$_2$	[IrCl(COD){Ir(μ-**1′′c**)(COD)}]·CH$_2$Cl$_2$	[IrCl(COD){Ir(μ-**1′b**)(COD)}]·C$_2$H$_4$Cl$_2$	[IrCl(COD){Ir(μ-**1′′b**)(COD)}]	[Ir(**1′a**)(COD)]
Chemical formula	$C_{29}H_{35}Cl_7N_4Rh_2$	$C_{31}H_{42}Cl_4N_4Rh_2$	$C_{31}H_{41}Cl_3Ir_2N_4$	$C_{31}H_{41}Cl_3Ir_2N_4$	$C_{29}H_{37}ClIr_2N_4$	$C_{19}H_{21}IrN_4$
Formula mass	893.58	818.30	960.43	960.43	861.47	497.60
Crystal system	monoclinic	monoclinic	triclinic	triclinic	monoclinic	triclinic
Space group	$P2_1/c$	$P2_1/n$	P-1	P-1	$P2_1/n$	P-1
a/Å	11.6201(4)	16.4188(4)	11.0198(6)	10.6140(5)	12.4381(8)	11.1722(4)
b/Å	21.3123(8)	12.0285(4)	12.1754(7)	12.7787(6)	10.3211(5)	12.1332(4)
c/Å	14.0654(5)	16.8235(4)	12.5769(7)	12.3679(6)	21.1192(13)	12.4387(4)
α/°	90	90	69.998(4)	70.872(4)	90	90.363(3)
β/°	107.256(3)	96.462(2)	75.255(5)	87.496(4)	106.060(5)	101.469(3)
γ/°	90	90	89.537(5)	75.520(4)	90	102.790(3)
V/Å^3	3326.5(2)	3301.42(16)	1527.64(16)	1533.20(13)	2605.4(3)	1609.22(10)
Z	4	4	2	2	4	4
Crystal size/mm	0.34×0.29×0.26	0.15×0.11×0.08	0.41×0.15×0.01	0.12×0.08×0.05	0.16×0.09×0.06	0.15×0.08×0.02
μ/mm^{-1}	1.582	1.351	19.249	8.961	10.335	16.111
F(000)	1784.0	1656.0	920.0	920.0	1640.0	960.0
Absorption correction	integration	multi-scan	multi-scan	multi-scan	multi-scan	multi-scan
T_{min}/T_{max}	0.6295/0.6999	0.5558/0.9127	0.0609/1.0000	0.2533/0.7013	0.3659/0.5687	0.1407/0.6980
Θ range/°	1.792–26.000	1.643–26.837	3.878–67.686	1.983–32.450	1.722–26.877	3.631–68.968
No. of refls. measured	15474	21980	11695	15324	11183	14038
Independent refls. [R_{int}]	6511 [0.0229]	7009 [0.0218]	5595 [0.0339]	9179 [0.0393]	5327 [0.0326]	5845 [0.0291]
Parameters	396	406	365	363	327	435
Final R_1 (wR_2) [$I > 2\sigma(I)$]	0.0248 (0.0586)	0.0333 (0.0812)	0.0519 (0.1652)	0.0286 (0.0668)	0.0492 (0.0936)	0.0409 (0.1209)
Final R_1 (wR_2) [all data]	0.0301 (0.0606)	0.0411 (0.0862)	0.0554 (0.1752)	0.0431 (0.0716)	0.0731 (0.1159)	0.0424 (0.1231)
Residual electron density/eÅ^{-3}	−0.595/0.825	−0.764/0.684	−3.154/2.171	−1.539/3.266	−2.848/1.930	−1.787/1.585
Goodness of fit	1.054	1.041	1.225	1.031	1.139	1.122

parameter of their bonding partner. Experimental details for each diffraction experiment are given in Table 2.

Crystallographic data (excluding structure factors) for the structures in this paper have been deposited with the Cambridge Crystallographic Data Centre, CCDC, 12 Union Road, Cambridge CB21EZ, UK. Copies of the data can be obtained free of charge on quoting the depository numbers CCDC-2039623 ([RhCl(COD){Rh(μ-**1'a**)(COD)}]·2$CHCl_3$), CCDC-2039624 ([{RhCl(COD)}$_2$(μ-**1cH**)]·CH_2Cl_2), CCDC-2039625 ([IrCl(COD){Ir(μ-**1''c**)(COD)}]·CH_2Cl_2), CCDC-2039626 ([IrCl(COD){Ir(μ-**1'b**)(COD)}]·$C_2H_4Cl_2$), CCDC-2039627 ([IrCl(COD){Ir(μ-**1''b**)(COD)}]), and CCDC-2039628 ([Ir(**1'a**)(COD)]) (Fax: +44-1223-336-033; E-Mail: deposit@ccdc.cam.ac.uk, http://www.ccdc.cam.ac.uk).

Supporting Information (see footnote on the first page of this article): Plots of NMR spectra (Figures S1–S12).

Acknowledgements

Open access funding enabled and organized by Projekt DEAL.

Keywords: Carbenes · Coordination modes · Iridium; Rhodium · X-ray diffraction

[1] C. A. Ramsden, *Tetrahedron* **2013**, *69*, 4146–4159.
[2] a) K. Kureja, J. Zinke, C. Bruhn, U. Siemeling, *Chem. Commun.* **2019**, *55*, 9705–9708; for closely related benzimidazolium-benzimidazolates, see: b) K. Kureja, C. Bruhn, M. R. Ringenberg, U. Siemeling, *Inorg. Chem.* **2019**, *58*, 16256–16266.
[3] a) C. Färber, M. Leibold, C. Bruhn, M. Maurer, U. Siemeling, *Chem. Commun.* **2012**, *48*, 227–229; for a Nitron homologue, see: b) C. Thie, C. Bruhn, M. Leibold, U. Siemeling, *Molecules* **2017**, *22*, 1133.
[4] For closely related betaine–carbene tautomerisations, see: a) A. A. Danopoulos, A. Massard, G. Frison, P. Braunstein, *Angew. Chem. Int. Ed.* **2018**, *57*, 14550–14554; b) J. Zhang, E. G. Hübner, J. C. Namyslo, M. Nieger, A. Schmidt, *Org. Biomol. Chem.* **2018**, *16*, 6801–6808; c) N. Pidlypnyi, S. Wolf, M. Liu, K. Rissanen, M. Nieger, A. Schmidt, *Tetrahedron* **2014**, *70*, 8672–8680; d) A. A. Danopoulos, P. Braunstein, *Chem. Commun.* **2014**, *50*, 3055–3057; e) N. Pidlypnyi, F. Uhrner, M. Nieger, M. H. H. Drafz, E. G. Hübner, J. C. Namyslo, A. Schmidt, *Eur. J. Org. Chem.* **2013**, 7739–7748; f) N. Pidlypnyi, J. C. Namyslo, M. H. H. Drafz, M. Nieger, A. Schmidt, *J. Org. Chem.* **2013**, *78*, 1070–1079; g) A. A. Danopoulos, K. Yu, Monakhov, P. Braunstein, *Chem. Eur. J.* **2013**, *19*, 450–455; h) V. César, J.-C. Tourneux, N. Vujkovic, R. Brousses, N. Lugan, G. Lavigne, *Chem. Commun.* **2012**, *48*, 2348–2351.
[5] Reviews on NHC–betaine interconversions: a) B. Stanovnik, *Adv. Heterocycl. Chem.* **2016**, *119*, 209–239; b) A. Schmidt, S. Wiechmann, C. F. Otto, *Adv. Heterocycl. Chem.* **2016**, 119, 143–172; c) A. Schmidt, S. Wiechmann, T. Freese, *Arkivoc* **2013**, *i*, 424–469.
[6] Seminal papers: a) L. P. Spencer, S. Winston, M. D. Fryzuk, *Organometallics* **2004**, *23*, 3372–3374; b) R. E. Douthwaite, J. Houghton, B. M. Kariuki, *Chem. Commun.* **2004**, 698–699; c) P. L. Arnold, S. A. Mungur, A. J. Blake, C. Wilson, *Angew. Chem. Int. Ed.* **2003**, *42*, 5981–5984; *Angew. Chem.* **2003**, *115*, 6163–6166.
[7] Selected reviews: a) A. Nasr, A. Winkler, M. Tamm, *Coord. Chem. Rev.* **2016**, *316*, 68–124; b) S. T. Liddle, I. S. Edworthy, P. L. Arnold, *Chem. Soc. Rev.* **2007**, *36*, 1732–1744; c) H. M. Lee, C.-C. Lee, P.-Y. Cheng, *Curr. Org. Chem.* **2007**, *11*, 1491–1524.
[8] a) R. Savka, H. Plenio, *Dalton Trans.* **2015**, *44*, 891–893; for seminal papers concerning this "weak base approach", see: b) O. Santoro, A. Collado, A. M. Z. Slawin, S. P. Nolan, C. Cazin, *Chem. Commun.* **2013**, *49*, 10483–10485; c) R. Visbal, A. Laguna, C. Gimeno, *Chem. Commun.* **2013**, *49*, 5642–5644; d) A. Collado, A. Gómez-Suárez, A. R. Martin, A. M. Z. Slawin, S. P. Nolan, *Chem. Commun.* **2013**, *49*, 5541–5543; e) S. Zhu, R. Liang, H. Jiang, *Tetrahedron* **2012**, *68*, 7949–7955; f) B. Landers, O. Navarro, *Eur. J. Inorg. Chem.* **2012**, 2980–2982.
[9] Seminal paper: a) H. M. J. Wang, I. J. B. Lin, *Organometallics* **1998**, *17*, 972–975.
[10] Reviews: a) J. C. Y. Lin, R. T. W. Huang, C. S. Lee, A. Bhattacharyya, W. S. Hwang, I. J. B. Lin, *Chem. Rev.* **2009**, *109*, 3561–3598; b) I. J. B. Lin, C. Sekhar Vasam, *Coord. Chem. Rev.* **2007**, *251*, 642–670.
[11] For a recent review, see: a) I. Haiduc, *J. Coord. Chem.* **2019**, *72*, 2127–2159; for early structurally characterised examples, see: b) G. Kolks, S. J. Lippard, *Acta Crystallogr. Sect. C* **1984**, *40*, 261–271; c) Y. Huawa, S. Juen, C. Liaorong, L. Baosheng, *Polyhedron* **1996**, *15*, 3891–3895.
[12] Reviews: a) M. Brookhart, M. L. H. Green, G. Parkin, *Proc. Natl. Acad. Sci. USA* **2007**, *104*, 6908–6914; b) L. Brammer, *Dalton Trans.* **2003**, 3145–3157.
[13] Selected reviews: a) L. M. Eitel, H. A. Fargher, M. M. Haley, D. W. Johnson, *Chem. Commun.* **2019**, *55*, 5195–5206; b) J. Cai, J. L. Sessler, *Chem. Soc. Rev.* **2014**, *43*, 6198–6213; c) G. R. Desiraju, T. Steiner, *The Weak Hydrogen Bond in Structural Chemistry and Biology*, Oxford University Press, Oxford, **1999**; see also: d) V. Balamurugan, M. Singh Hundal, R. Mukherjee, *Chem. Eur. J.* **2004**, *10*, 1683–1690; e) C. B. Aakeröy, T. A. Evans, K. R. Seddon, I. Pálinkó, *New J. Chem.* **1999**, 145–152; f) G. Aullón, D. Bellamy, L. Brammer, E. A. Bruton, A. G. Orpen, *Chem. Commun.* **1998**, 653–654; g) R. Taylor, O. Kennard, *J. Am. Chem. Soc.* **1982**, *104*, 5063–5070.
[14] Selected recent reviews: a) Á. Vivancos, C. Segarra, M. Albrecht, *Chem. Rev.* **2018**, *118*, 9493–9586; b) D. Munz, *Organometallics* **2018**, *37*, 275–289; c) M. Albrecht, *Adv. Organomet. Chem.* **2014**, *62*, 111–158; d) R. H. Crabtree, *Coord. Chem. Rev.* **2013**, *257*, 755–766; e) O. Schuster, L. Yang, H. G. Raubenheimer, M. Albrecht, *Chem. Rev.* **2009**, *109*, 3445–3478; see also:; f) J. B. Waters, J. M. Goicoechea, *Coord. Chem. Rev.* **2015**, *293–294*, 80–94.
[15] Seminal paper: S. Gründemann, A. Kovacevic, M. Albrecht, J. W. Faller, R. H. Crabtree, *J. Am. Chem. Soc.* **2002**, *124*, 10473–10481.
[16] a) A. Kumar, S. Semwal, J. Choudhury, *ACS Catal.* **2019**, *9*, 2164–2168; b) S. Garhwal, B. Maji, S. Semwal, J. Choudhury, *Organometallics* **2018**, *37*, 4720–4725; c) S. Semwal, A. Kumar, J. Choudhury, *Catal. Sci. Technol.* **2018**, *8*, 6137–6142. For closely related work using a pyridine-based "remote" instead of an imidazole-based "abnormal" NHC units, see: d) S. Semwal, J. Choudhury, *Angew. Chem. Int. Ed.* **2017**, *56*, 5556–5560; *Angew. Chem.* **2017**, *129*, 5648–5652; e) S. Semwal, J. Choudhury, *ACS Catal.* **2016**, *6*, 2424–2428.
[17] Selected reviews: a) D. F. Fernández, J. L. Mascareñas, F. López, *Chem. Soc. Rev.* **2020**, *49*, 7378–7405; b) C. Slugovc, I. Pardilla-Martínez, S. Sirol, E. Carmona, *Coord. Chem. Rev.* **2001**, *213*, 129–157.
[18] M. Viciano, M. Poyatos, M. Sanaú, E. Peris, A. Rossin, G. Ujaque, A. Lledós, *Organometallics* **2006**, *25*, 1120–1134.
[19] B. Cordero, V. Gómez, A. E. Platero-Prats, M. Revés, J. Echeverría, E. Cremades, F. Barragán, S. Alvarez, *Dalton Trans.* **2008**, 2832–2838.
[20] J. Harada, M. Harakawa, K. Ogawa, *Acta Crystallogr. Sect. B* **2004**, *60*, 578–588.

[21] T. G. Appleton, H. C. Clark, L. E. Manzer, *Coord. Chem. Rev.* **1973**, *10*, 335–422.
[22] See, for example: a) K. A. Netland, A. Krivikapic, M. Tilset, *J. Coord. Chem.* **2010**, *63*, 2909–2927; b) J. Slattery, R. J. Thatcher, Q. Shi, R. E. Douthwaite, *Pure Appl. Chem.* **2010**, *82*, 1663–1671; c) M. Heckenroth, A. Neels, M. G. Garnier, P. Aebi, A. W. Ehlers, M. Albrecht, *Chem. Eur. J.* **2009**, *15*, 9375–9386.
[23] M. J. Page, J. Wagler, B. A. Messerle, *Dalton Trans.* **2009**, 7029–7038.
[24] pK_a values <24 in DMSO have been determined for Arduengo type NHC precursors and their ring-expanded relatives, whereas corresponding aNHC precursors typically have pK_a values >30; see: a) N. Konstandaras, M. H. Dunn, E. T. Luis, M. C. Cole, J. B. Harper, *Org. Biomol. Chem.* **2020**, *18*, 1910–1917; b) Z. Whang, X.-S. Xue, Y. Fu, P. Ji, *Chem. Asian J.* **2020**, *15*, 169–181. For comparison, p$K_a=24.2$ in DMSO has been reported for $[Ag_2OH]^+$; see: c) J. M. Hayes, M. Viciano, E. Peris, G. Ujaque, A. Lledós, *Organometallics* **2007**, *26*, 6170–6183.
[25] E. Alcalde, I. Dinarés, J. Frigola, C. Jaime, J.-P. Fayet, M.-C. Vertut, C. Miravitlles, J. Rius, *J. Org. Chem.* **1991**, *56*, 4223–4233.
[26] G. M. Sheldrick, *Acta Crystallogr., Sect. A: Found. Crystallogr.* **2008**, *64*, 112–122.

Manuscript received: October 26, 2020
Revised manuscript received: November 18, 2020
Accepted manuscript online: November 19, 2020

